

Provided for non-commercial research and educational use only.  
Not for reproduction or distribution or commercial use.



This article was originally published in a journal published by Elsevier, and the attached copy is provided by Elsevier for the author's benefit and for the benefit of the author's institution, for non-commercial research and educational use including without limitation use in instruction at your institution, sending it to specific colleagues that you know, and providing a copy to your institution's administrator.

All other uses, reproduction and distribution, including without limitation commercial reprints, selling or licensing copies or access, or posting on open internet sites, your personal or institution's website or repository, are prohibited. For exceptions, permission may be sought for such use through Elsevier's permissions site at:

<http://www.elsevier.com/locate/permissionusematerial>



## Nanostructured magnetizable materials that switch cells between life and death

Thomas R. Polte<sup>a</sup>, Mengyan Shen<sup>b</sup>, John Karavitis<sup>a</sup>, Martin Montoya<sup>a</sup>, Jay Pendse<sup>a</sup>, Shannon Xia<sup>a</sup>, Eric Mazur<sup>b</sup>, Donald E. Ingber<sup>a,\*</sup>

<sup>a</sup>*Vascular Biology Program, Departments of Pathology and Surgery, Children's Hospital and Harvard Medical School, Boston, MA, USA*

<sup>b</sup>*Department of Physics, Division of Engineering and Applied Sciences, Harvard University, Cambridge, MA, USA*

Received 6 November 2006; accepted 25 January 2007

Available online 15 February 2007

### Abstract

Development of biochips containing living cells for biodetection, drug screening and tissue engineering applications is limited by a lack of reconfigurable material interfaces and actuators. Here we describe a new class of nanostructured magnetizable materials created with a femtosecond laser surface etching technique that function as multiplexed magnetic field gradient concentrators. When combined with magnetic microbeads coated with cell adhesion ligands, these materials form microarrays of 'virtual' adhesive islands that can support cell attachment, resist cell traction forces and maintain cell viability. A cell death (apoptosis) response can then be actuated on command by removing the applied magnetic field, thereby causing cell retraction, rounding and detachment. This simple technology may be used to create reconfigurable interfaces that allow users to selectively discard contaminated or exhausted cellular sensor elements, and to replace them with new living cellular components for continued operation in future biomedical microdevices and biodetectors.

© 2007 Elsevier Ltd. All rights reserved.

**Keywords:** Magnetic particles; Magnetic gradient concentrator; Culture substrate; Apoptosis; Mechanical force; Cell shape

### 1. Introduction

The development of microchips containing biological molecules, such as multiplexed arrays of specific DNA sequences, has revolutionized genomics, diagnostics and pathogen detection. In the future, it is likely that living cells will be integrated as system components within biochip-based microdevices used for drug development, medical microdevices and biodetection because of their unique abilities to simultaneously sense and respond to multiple physiological or pathological stimuli. However, biocompatible cell–material interfaces will need to be created to make these technologies a reality.

Microfabrication techniques, such as soft lithography and microcontact printing, have been used to create arrays of adhesive islands that may be used to place cells in predefined positions and maintain them in a functional

state [1–3]. These substrates also have been integrated with microfluidic systems that permit cells to be plated on these substrates and nutrient media to be delivered continuously to maintain cell function and to introduce various chemical stimuli [4–6]. But these systems are limited in that they are not reconfigurable. For example, it would be extremely desirable to have future biodetectors containing cells that can be rapidly removed and replaced with new cellular components after exposure to contagious biopathogens in order to reboot the device without requiring addition of expensive enzymes or harsh chemicals that might interfere with the functionality of the system. This type of reconfigurable functionality also might be useful for future drug screening, tissue engineering and biocomputational applications in which living cells are used as primary signal processing elements [7–9].

Several systems have been described that allow users to control the cell adhesive properties of substrates, including thermal responsive polymer surfaces [10], photo-initiated gels [11,12] and electrochemical modulation of

\*Corresponding author. Tel.: +1 617 919 2223; fax: +1 617 730 0230.

E-mail address: [donald.ingber@childrens.harvard.edu](mailto:donald.ingber@childrens.harvard.edu) (D.E. Ingber).

self-assembled monolayers [13,14]. Although these technologies may provide useful methods to rapidly actuate changes in substrate adhesivity and cell behavior, they are not easily reversed within an existing microsystem. Here we describe a microsystem in which cell adhesion, position and viability can be controlled magnetically to meet this challenge.

## 2. Materials and methods

### 2.1. Nanofabrication of magnetic gradient concentrators

Arrays of silicon nanospikes were fabricated by femtosecond laser etching, as previously reported [15]. Briefly, silicon chips [flat zone Si(111)] were masked with 2  $\mu\text{m}$ -thick copper transmission electron microscope grids with hexagonal opening widths of 30  $\mu\text{m}$ . The chips were mounted normal to the laser beam on a three-axis translation stage in a vacuum chamber with a base pressure of less than  $10^{-2}$  Pa. Laser pulses (800 nm, 100 fs at 0.3 mJ) were focused to a beam waist of 200  $\mu\text{m}$  on the sample surface. Samples were translated relative to the laser beam vertically at a speed of 200  $\mu\text{m}/\text{s}$  to irradiate the entire surface. Laser-etched silicon chips were subsequently coated with a thin (450  $\text{\AA}$ ) layer of magnetizable cobalt using a SHARON TE-4 four-source thermal evaporation system. After irradiation and coating, the resulting structures were imaged with a scanning electron microscope.

Arrays of stainless steel nanospikes were fabricated by femtosecond laser etching of surgical stainless steel blades (#21, Becton Dickinson, Franklin Lakes, NJ) that were mechanically precut into 1  $\text{cm}^2$  wafers. To create patterned arrays, the surface was polished with a diamond lapping film, and then mounted normal to the laser beam on a three-axis translation stage in a vacuum chamber with a base pressure of less than  $10^{-2}$  Pa. Laser pulses (800 nm, 100 fs at 0.015 mJ) were focused on the sample surface, and the sample was translated relative to the laser beam vertically at a speed of 500  $\mu\text{m}/\text{s}$  to etch parallel linear valleys with separation of approximately 100  $\mu\text{m}$  (center to center) on the surface of the stainless steel. The sample was translated 90° and linear etching was repeated to generate cross-hatched valleys, leaving an array of square raised areas with sides approximately 50  $\mu\text{m}$  in length.

To create nanospikes on the raised square arrays, wafers were again lightly polished with a diamond lapping film, and then cleaned with acetone followed by a methanol rinse. Wafers were subsequently placed in a glass container, mounted on a three-axis translation stage and filled with distilled water. The surface of the array was irradiated by a 1 kHz train of 100 fs, 80  $\mu\text{J}$  pulses at 400 nm wavelength from a frequency-doubled, amplified titanium:sapphire laser. The laser pulses were focused by a 0.25-m focal-length lens and traveled through 10 mm of water before striking the surface at normal incidence. The focal point is about 10 mm behind the surface and the spatial profile of the laser spot is nearly Gaussian, with a fixed beam waist of 60  $\mu\text{m}$  at the sample surface. The sample was translated relative to the laser beam at a speed of 200  $\mu\text{m}/\text{s}$  to create nanospikes over the entire micro-arrayed surface. The dimensions of the resulting structures were determined from scanning electron microscope images as well as analysis with a Dektak 6M profilometer.

Etched stainless steel wafers were coated with Sylgard 184 polydimethylsiloxane (PDMS; Dow Corning, Midland, MI) using a G3P-8 Spincoat device (Specialty Coating Systems/Cookson Electronics, Indianapolis, IN) to prevent surface oxidation and optimize biocompatibility. PDMS base and curing agents were mixed in a 10:1 ratio, degassed by vacuum for 30 min, spin-cast, and cured at least 3 h at 60 °C. Cured PDMS surfaces were made hydrophilic by 8 min exposure to an oxidizing plasma in an UVO-Cleaner 342 (Jelight, Irvine, CA), and wafers were immediately immersed in aqueous Pluronic F-127 solution (1 g/L; BASF, Mount Olive, NJ) for 1 h at room temperature to resist cell adhesion [16]. Wafers were rinsed extensively in phosphate buffered saline prior to incubation with beads and/or cells. The thickness of the PDMS was estimated to be 5  $\mu\text{m}$  based on confocal imaging of coated wafers in which 200 nm green fluorescent beads were added to the PDMS.

### 2.2. Experimental system

Immortalized human umbilical vein endothelial (HUVE) cells that stably expressed green fluorescent protein (GFP) [17] were cultured in EBM medium (Cambrex) supplemented with EGM-2 MV growth factor supplement (Cambrex) at 37 °C and 5%  $\text{CO}_2$ . Subconfluent cells were detached by trypsinization, washed once in medium and cultured in EBM containing EGM-2 MV on magnetic substrates. Tosyl-activated superparamagnetic microbeads (4.5  $\mu\text{m}$  diameter; Dynal Biotech, Oslo, Norway) were coated with an RGD-containing peptide (50  $\mu\text{g}/\text{ml}$ ; PepTite-2000; Integra LifeSciences, Plainsboro, NJ), that mediates cell adhesion through cell surface integrin receptors, as previously described [18,19].

Nanospike magnetic concentrators were placed horizontally in a cell culture apparatus that allowed permanent ceramic magnet cylinders (27 MG Oe; Polysciences Inc., Warrington, PA) to be placed directly beneath the concentrators, separated only by thin cover glass (No. 0; Dow Corning). For bead patterning, 100,000 RGD-coated beads were added to each magnetic field concentrator in 10 mm diameter cloning cylinders (Bellco Biotechnology, Vineland, NJ) to avoid dilution of beads in the larger medium reservoir. Beads were readily visualized by fluorescence microscopy due to their auto-fluorescence in the Texas-Red channel. Cells were added to magnetic substrates (2500 cells/substrate) in 10 mm diameter cloning cylinders, and placed in a culture incubator at 37 °C under 5%  $\text{CO}_2$  for the indicated times. In some experiments, cells were allowed to bind to the RGD-beads (20 beads/cell) in suspension for 30 min at 37 °C prior to adding them to the magnetic field concentrators. Changes in projected cell areas were measured using computerized image analysis as previously described [1,18]; this was facilitated by visualizing the GFP-labeled HUVE cells using fluorescence microscopy.

The magnetic field gradient concentrators were calibrated by pulling 4.5  $\mu\text{m}$  diameter beads through a glycerol solution of known viscosity (1000 cP), as previously described [20]. Briefly, bead displacements and velocities were quantitated using IPLab image analysis software and time-lapse brightfield images (<0.1 s intervals) captured with a Nikon Diaphot 300 inverted microscope and a Photometrics CoolSnap HQ CCD digital camera. After recording the beads' velocities through the fluid, Stokes' formula for low Reynolds number flow was used to deduce the forces [ $\text{Force} = 3\pi\eta Dv$ , where  $\eta$  is the viscosity of the fluid,  $D$  is the bead diameter, and  $v$  is the velocity of the bead through the fluid]. For force calibration experiments, magnetic field gradient concentrators were placed on edge in glass-bottomed culture dishes, such that beads could be tracked in the  $X$ - $Y$  plane of the microscope field as they approached the surface of the magnetic field gradient concentrator. Forces on individual beads were plotted against the distance between the bead and the surface of the magnetic field gradient concentrator.

To measure apoptosis we used a TUNEL *in situ* cell death detection kit (Roche, Penzberg, Germany) that measures DNA fragmentation as an indicator of programmed cell death. To harvest cells for this assay, magnets were removed from concentrators to release cells and cells were transferred to poly-D-lysine (Sigma) coated 4-chamber slides (Lab-Tek, Naperville, IL). Cells were allowed to adhere to the slides for 30 min and then fixed for 1 h in 4% paraformaldehyde in PBS. Apoptosis-associated DNA strand breakage was identified by following the TUNEL assay kit protocol for adherent cells, and cells were counterstained with DAPI to visualize all nuclei. Positive staining was detected by fluorescence microscopy using a Nikon Diaphot 300 inverted microscope and a Photometrics CoolSnap HQ CCD digital camera, and images were captured and analyzed with IPLab software. At least 100 cells were counted for each condition and results are presented as a percentage of DAPI-stained nuclei that exhibited positive TUNEL staining.

## 3. Results

The goal of this study was to microfabricate a cell culture environment containing a reconfigurable material interface that can rapidly actuate changes in substrate adhesivity

and cell behavior. Our design concept was based on past work which showed that anchorage-dependent cells, such as endothelial cells, require adhesion to substrates that can resist cell traction forces and produce a minimal degree of cell distortion to maintain cell viability and suppress the cellular suicide program (apoptosis) [1,21]. To distort their shape and avoid entry into the apoptosis pathway, anchorage-dependent cells must exert substantial force ( $> 1 \text{ nN}/\mu\text{m}^2$ ) against their individual focal adhesions to the underlying extracellular matrix (ECM) [22–24]. This range of force can be applied to cells using magnetic microparticles coated with ECM ligands [25,26], and forces applied over integrins in this manner have been shown to alter intracellular biochemical activities including translation, signal transduction and gene expression [20,27–29]. This observation raised the possibility of creating a ‘virtual’ adhesive substrate by exerting forces on cell surface integrin-bound magnetic beads using applied magnetic fields that are of sufficient strength to resist cell tractional forces, and thereby maintain cell adhesion and viability; removal of the applied magnetic field would then induce cell retraction, rounding and death (Fig. 1). Importantly, this system could then be reconfigured by adding new beads and cells, thus providing a significant advantage over past materials that, for example, promote substrate release and cell detachment by altering cell temperature [10]. However, to produce pulling forces magnetically, it is necessary to create very high local magnetic field gradients. To do this in a manner that would be useful for future cell-based microdevices where single cell analysis may be required, we needed to generate these in a multiplexed

manner with each adhesive magnetic island being on the scale of a single cell.

Regions of magnetic materials with higher curvature exhibit enhanced magnetic field gradients [30]. We have previously shown that irradiation of the surface of a silicon chip with a high power femtosecond laser (800 nm, 100 fs, 0.3 mJ) in the presence of certain gases, such as  $\text{SF}_6$ , transforms its flat mirror-like surface into a forest of microscopic spikes with very high curvature in the nanometer to low micrometer range [15,31]. Thus, we explored whether these novel laser-etched silicon chips could enhance local magnetic field gradients if coated with a layer of magnetizable material, and if so, whether microarrays of cell-sized islands could be created with this technique.

In our initial studies, arrays of multiple, micrometer-sized islands of high density nanospikes were etched into silicon substrates by masking the chips with a copper transmission electron microscopy (TEM) grid containing  $30 \mu\text{m}$  wide hexagonal openings during laser ablation (Fig. 2a). The substrates were then coated with a thin (450 Å) layer of Cobalt by thermal evaporation to render these substrates magnetizable. When a permanent ceramic magnet (27 MG Oe, Polysciences Inc.) was placed beneath the etched silicon wafer and fluorescent superparamagnetic microbeads ( $4.5 \mu\text{m}$  diameter; Dynal) were added to its surface in tissue culture medium, the beads preferentially

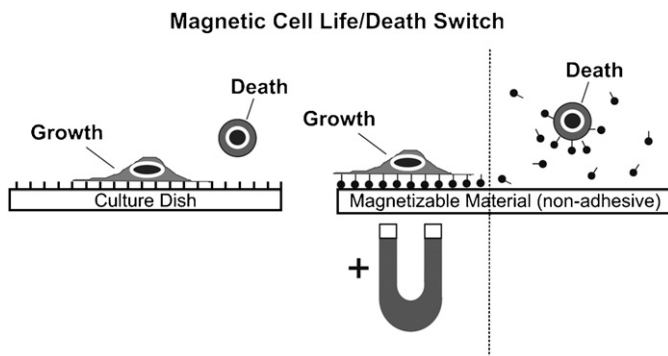


Fig. 1. Schematics showing substrates that support cell adhesion and control cell viability. (Left) Anchorage-dependent cells, such as HUVE cells, normally must attach and spread on a rigid ECM-coated culture substrate in order to survive and grow; cells that pull themselves off of a poorly adhesive substrate and round undergo apoptosis. (Right) Schematic of the reconfigurable magnetic control system for switching cells between cell life and death that is described here. Cells are allowed to adhere to ECM-coated microbeads that bind their cell surface adhesion (integrin) receptors. In the presence of a high local magnetic field gradient, magnetic forces exerted on the beads will pull them down onto the surface of a non-adhesive substrate and create a ‘virtual’ cell adhesive island. If the force is great enough to resist cell traction forces, the cells will spread and remain viable. When the magnetic field is removed, the cells will retract the beads, round and switch on a cellular suicide program.

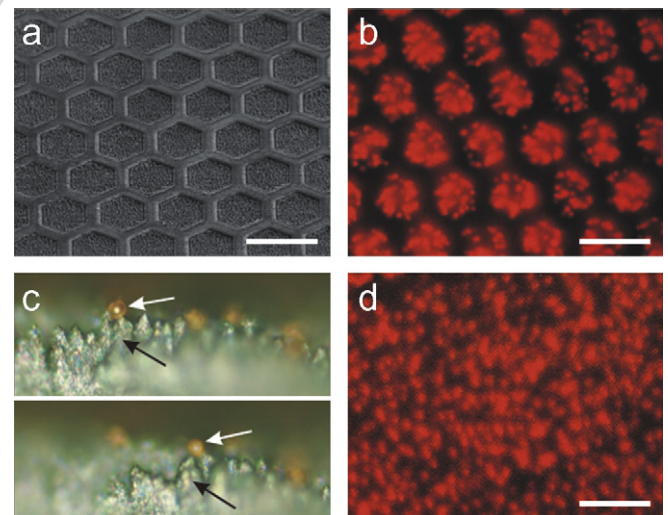


Fig. 2. A multiplexed magnetic field gradient concentrator fabricated by femtosecond laser etching of a silicon wafer. (a) Low power scanning electron micrograph of the cobalt-coated, laser-etched surface of a silicon wafer. Arrays of microspikes contained within hexagonal regions were created using a copper transmission electron microscope grid as a mask during the laser etching process. (b) Fluorescence micrograph showing that fluorescent superparamagnetic microbeads ( $4.5 \mu\text{m}$  diameter) are pulled to the hexagonal nanospike regions of the microarray in the presence of an applied magnetic field. (c) High power micrograph of  $4.5 \mu\text{m}$  beads (white arrow) that localize preferentially to the apex of the nanospikes (black arrow). (d) Fluorescence image showing that the magnetic microbeads exhibit a random distribution on the unpatterned regions of these cobalt-coated silicon wafers in the presence of a magnetic field (bar,  $50 \mu\text{m}$ ).

attracted to the hexagonal islands containing the nanopikes (Fig. 2b). Higher resolution light microscopic analysis of etched substrates placed on edge and viewed from the side confirmed that the beads were specifically attracted to the apex of the cobalt-coated nanopikes that exhibited the highest curvature (Fig. 2c). In contrast, no patterning of magnetic beads was observed when they were placed on a smooth cobalt-coated silicon chip in the presence (Fig. 2d) or absence (not shown) of an external magnet.

To increase the durability and magnetic conductance of these magnetic concentrators, as well as to eliminate the necessity of coating with cobalt, we explored whether magnetizable stainless steel substrates could be used in place of silicon wafers. Preliminary characterization of laser-irradiated stainless steel (using a surgical scalpel blade) revealed that nanopikes formed slightly below the plane of the steel surface (not shown), whereas on silicon, laser irradiation results in nanopikes that project above the plane of the surface. To present the nanopiked regions above the plane of the steel surface, we etched 2  $\mu\text{m}$  deep valleys in a square (50  $\times$  50  $\mu\text{m}$ ) grid pattern by using a computer to precisely control translational movements of planar steel substrates in the path of 800 nm, 100 fs laser pulses in a vacuum (Figs. 3a and b). The remaining raised square surfaces of these etched steel substrates were then irradiated in water with 400 nm, 100 fs laser pulses to produce nanopikes in these elevated regions (Fig. 3c). This resulted in creation of a magnetizable stainless steel surface containing 50  $\times$  50  $\mu\text{m}$  elevated square mesas separated by 50  $\mu\text{m}$  wide valleys at a depth of 2  $\mu\text{m}$  (Fig. 3d). Analysis of high power images of regions within the elevated islands revealed that the steel nanopikes were on average

282  $\pm$  5 nm (S.E.M.) wide and 715  $\pm$  23 nm high, with a center-to-center spacing of 406  $\pm$  78 nm (Fig. 3e).

The steel nanostructured island microarrays were spin-coated with a thin layer ( $\sim$ 5  $\mu\text{m}$ ) of PDMS to create a flat surface and prevent metal oxidation in the aqueous medium, thereby further increasing biocompatibility. The PDMS surface was subsequently treated with Pluronic F-127 to make the surface non-adhesive to cells, cell-derived ECM proteins, or the magnetic beads. These substrates were placed in modified tissue culture dishes that allowed for permanent ceramic magnets to be placed directly beneath the magnetic concentrators, separated by only a thin (80–130  $\mu\text{m}$  thick) glass coverslip that isolates the magnet from culture medium. When magnetic microbeads (4.5  $\mu\text{m}$  diameter; 1500 beads/ $\text{mm}^2$ ; Dynal) coated with the RGD cell binding peptide of fibronectin were added in medium in the absence of an applied magnet, they settled down onto the PDMS surface by gravity over a period of minutes but they did not distribute in any discernable pattern (Fig. 4a). In contrast, when the same beads were suspended over the nanostructured stainless steel device in the presence of a single ceramic magnet, virtually all of the beads were preferentially concentrated at sites directly over the square, regularly spaced, nanopiked islands of the microarray (Fig. 4b). Importantly, the beads distributed as a single layer across the entire region of the raised islands containing the nanopikes. With the magnet in place, beads remained in patterned arrays even after gentle medium changes. In contrast, after removing the underlying magnet, the beads were readily dislodged and easily removed by gentle swirling of the medium (not shown).

To quantify the forces exerted on individual beads (and hence, cells) by the stainless steel magnetic field gradient concentrator, we analyzed its ability to pull the magnetic beads through a high viscosity (1000 cP) glycerol solution. Stokes' law was used to calculate the applied force based on measured changes in bead displacement induced by the applied magnetic field, as previously described [20]. For these experiments, concentrators were placed vertically in glass-bottomed culture dishes so that the beads could be tracked in the  $X$ – $Y$  plane of the microscope field as they approached the surface of the stainless steel magnetic field gradient concentrator. These studies confirmed that

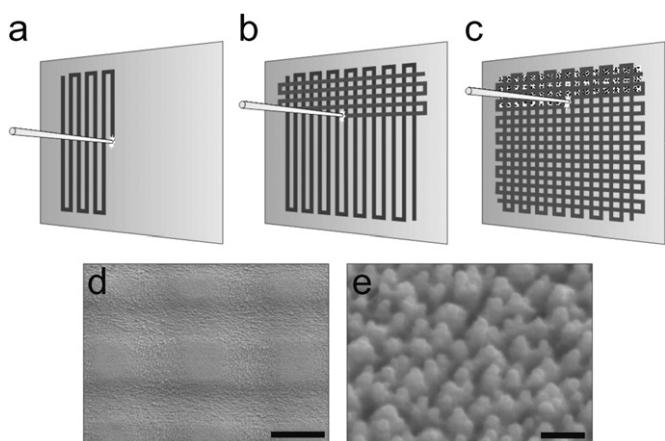


Fig. 3. Diagram describing the femtosecond laser etching method used to create microarrays of nanopike-covered islands on magnetizable stainless steel. (a), (b) A rectangular grid of valleys is first etched in the surface of the stainless steel substrate by laterally translating a laser beam (800 nm, 100 fs at 0.015 mJ) to create an array of raised square islands. (c) Femtosecond laser pulses (400 nm, 100 fs, 80  $\mu\text{mJ}$ ) are then applied to the raised squares to create nanopikes on these surfaces. Low (d) and high (e) power scanning electron micrographic views showing topography of the square arrays and individual nanopikes, respectively (bar, 50  $\mu\text{m}$  in (d) and 1  $\mu\text{m}$  in (e)).

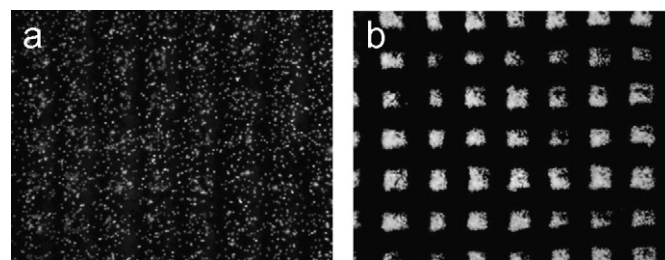


Fig. 4. Fluorescence images of magnetic microbeads added to a laser-etched, stainless steel, multiplexed, magnetic field concentrator in the absence (a) or presence (b) of an applied magnetic field.

individual magnetic microbeads were redirected specifically to the square elevated regions containing the nanospikes once they approached within approximately  $20\ \mu\text{m}$  of the nanoetched steel surface (Fig. 5a). Analysis of bead velocities resulted in reproducible force–distance relationships, and revealed that approximately  $0.25\text{--}2\ \text{nN}$  of force was applied to each magnetic bead within about  $20\ \mu\text{m}$  from the surface of the magnetic concentrator (Fig. 5b). As these force calibrations were performed with etched nanospike surfaces that were not coated with PDMS, the force generated at approximately  $5\ \mu\text{m}$  from the surface of the steel substrate corresponds to the force that would be experienced by the lowest layer of applied magnetic microbeads in the presence of PDMS. This force ranged from approximately  $0.9$  to  $1.3\ \text{nN}$  per bead for one magnet or two stacked magnets, respectively (Fig. 5b), which is in the range of the level of traction force living cells apply to individual focal adhesions [22–24].

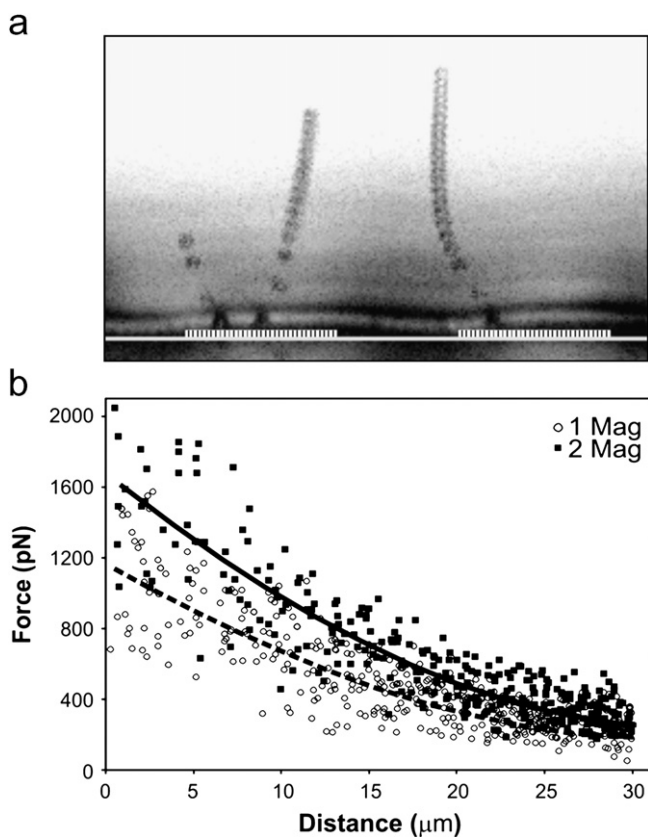


Fig. 5. Measurement of forces exerted on magnetic microbeads in close proximity to the magnetic field gradient concentrator. (a) Compilation of multiple bright field microscopic views taken at approximately  $0.5\ \text{s}$  time intervals showing the path taken by magnetic microbeads as they were tracked by time-lapse microscopy (while being pulled through glycerol toward magnetic gradient concentrator). Note changes in direction of beads towards nanospiked islands as they come to within close proximity to the nanostructured islands of the etched substrate (thin white rectangles). (b) Calculated relationship between distance and force as a function of varying the number of stationary ceramic magnets placed beneath the concentrator. Velocity measurements used to calculate applied forces based on Stokes' law were determined from images similar to those shown in (a).

To explore the utility of the stainless steel magnetic field concentrator as a magnetic cell culture substrate, RGD-coated microbeads were first added to multiple nanostructured square islands with a single ceramic magnet placed beneath the substrate. HUVE cells were plated on these magnetically stabilized microbead arrays at low density ( $40\ \text{cells}/\text{mm}^2$ ) to minimize cell–cell adhesion, and to limit more than one cell from adhering to each island of nanospikes. Cells adhered readily to the magnetically trapped beads that formed the ‘virtual’ adhesive islands, and some exhibited partial spreading (Fig. 6a). These results confirm that magnetic forces applied to the RGD-coated micromagnetic beads are sufficient to resist local cell traction forces (Fig. 6a). Cells that did not come into contact with beads remained non-adherent and were easily removed from the PDMS surface by gentle washing (not shown). In a separate experiment, cells were allowed to bind RGD-coated beads in suspension before the entire mixture was plated on the magnetic field concentrator substrate with a ceramic magnet below. These bead-bound cells also were efficiently pulled to the square nanospiked regions of the microarray (Fig. 6b). In both cases, the bead-bound cells maintained their position over the square islands of the microarray containing the nanospikes for the entire 2-day culture period, as long as the ceramic magnet remained in place during the study.

Computerized morphometric analysis of the projected areas of HUVE cells pre-bound to RGD-beads in suspension and cultured for 24 h in the presence of magnetic field gradient concentrators with 0, 1 or 2 stacked ceramic magnets placed beneath the substrate confirmed that cell spreading increased progressively (from  $386$  to  $526\ \mu\text{m}^2$ ) as the number of underlying ceramic magnets was raised from 0 to 2 (Fig. 7a). In contrast, all cells retracted and detached themselves from the surface of the PDMS-coated substrate when the magnets were removed

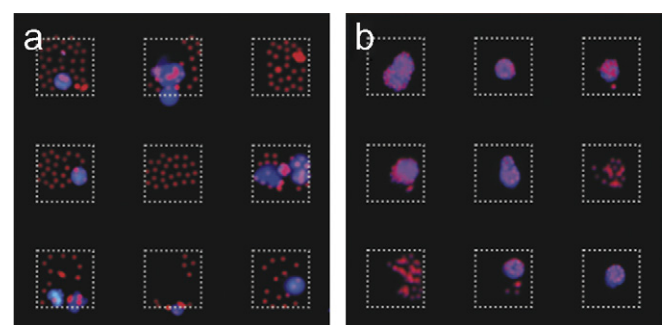


Fig. 6. Fluorescence micrographs showing micropatterning of cell adhesion within microarrays using the multiplexed magnetic gradient concentrator in combination with RGD-coated microbeads (a) HUVE cells expressing GFP (magenta) were allowed to settle by gravity onto RGD-coated magnetic microbeads (red) that had been previously pulled down to the surface of the magnetic gradient concentrator. (b) Cells that were pre-incubated with RGD-coated microbeads for 30 min in suspension prior to addition to the magnetic gradient concentrator. Note that cells preferentially localize to square islands containing raised nanospikes (dashed squares) using both techniques.

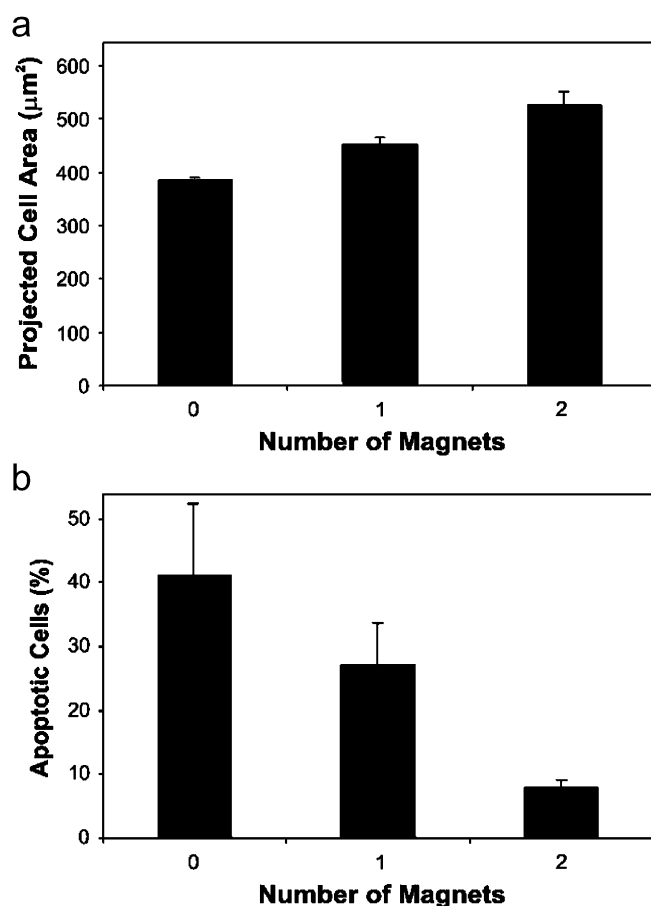


Fig. 7. Analysis of cell shape distortion (a) and apoptosis (b) in cells cultured on the multiplexed magnetic field gradient concentrator for 24 h in the presence of 0, 1 or 2 stacked stationary ceramic magnets. HUVE cells were allowed to bind to RGD-coated magnetic microbeads in suspension and then plated on the multiplexed magnetic field gradient concentrator. Projected cell areas were determined by computerized image analysis, and the percentage of apoptotic cells was quantitated using TUNEL staining. Note that addition of 2 magnets beneath the concentrator resulted in a statistically significant decrease in cell death as well as cell area ( $p < 0.04$ ).

(not shown). These findings confirm that in the presence of applied magnetic field gradients, these magnetically trapped magnetic beads do, in fact, form ‘virtual’ adhesive substrates that can resist cell traction forces in the absence of covalent linkage to the underlying rigid substrate.

HUVE cells rapidly switch on the cellular suicide program and undergo apoptosis if they are cultured in suspension or on adhesive substrates that cannot effectively resist cell traction forces and promote cell distortion [1,21]. Therefore, we explored whether removal of the magnet field gradient and associated cell rounding can be used to switch on the cellular suicide (apoptosis) program in this system. Importantly, analysis of apoptosis using the TUNEL assay to measure DNA fragmentation under the same conditions used to quantitate cell spreading (Fig. 7a) revealed a progressive increase in the percentage of cells undergoing cell death (from 8% to 41%; Fig. 7b) as the number of magnets was lowered from 3 to 0. These results

demonstrate that the magnetic field gradient concentrators can effectively resist cell traction forces so that cell distortion can be promoted, and cell viability can be maintained for at least 2 days in culture. They also show that cell death can be actuated simply by removing the applied magnetic field.

#### 4. Discussion

Taken together, these results demonstrate that multiplexed magnetic field gradient concentrators can be created using femtosecond laser etching technology, and that microarrays of ‘virtual’ cell adhesive islands can be created when these materials are combined with microbeads coated with cell adhesion ligands. In the presence of a magnetic field applied with an inexpensive stationary magnet, living cells can be cultured on these microarrays and be maintained in a viable state for days if provided with appropriate nutrients. If desired, the cells adherent to every island, or a subset of islands, can then be abruptly switched into a cell death program, and be physically washed away from the non-adhesive PDMS surface of the magnetic field concentrator without requirement of any enzymes (e.g., trypsin) or harsh chemicals. New beads and living cellular components may then be added through a microfluidic system to ‘reboot’ the system. All of the beads were coated with the same ligand and incubated with the same cell type in the present study. However, by covering these microarrays of virtual adhesive islands with an overlay that contains multiple microfabricated holes in corresponding positions that can be filled individually with different medium or cellular components using automated micropipetting techniques, this system can be provided with a combinatorial capability. These more sophisticated multiplexed systems would permit simultaneous analysis of the effects of multiple substrate ligands or soluble stimuli on multiple cell types.

The success of this reconfigurable technology required the development of magnetic field concentrators that enable these surfaces to trap micro- or nanoscale magnetic particles with sufficient force to resist cell generated traction forces. This was accomplished by adapting a femtosecond laser etching technique previously developed to create micro- and nanoscale spikes on flat silicon surfaces [15,31] to create magnetizable substrates that locally concentrate magnetic field gradients due to the high curvature of the spikes. By creating nanospikes on magnetizable stainless steel, we were able to increase magnetic conductance, durability, and biocompatibility of these substrates for studies with living cells, while minimizing cost.

Another important requirement for cellular microarray-based sensors is defined control of cell positioning and maintenance of this selectivity over time. This requires a surface that is resistant to adsorption of molecules and proteins present in the growth medium or secreted by the cells that might support cell adhesion. We were able to

inhibit protein adsorption by coating the surface of our devices with a uniform smooth layer of PDMS treated with Pluronic detergent, as previously described [16]. This technique proved highly effective for our purposes, as beads and cells were easily removed and replaced on these devices with extremely high fidelity of patterning, even after culturing cells for 2 days on the magnetic devices. In addition to this highly selective non-fouling support for bead and cell localization, the PDMS-coated, laser-etched microarrays concentrated beads in a uniform layer across the entire surface of each raised nanopiked area which likely helps to facilitate cell adhesion and spreading. An important procedural consideration to achieve this uniform distribution is that careful attention must be paid to the final density of beads on the magnetic field concentrators in order to avoid excessive bead towering on the magnetized nanopiked regions.

Although our experiments demonstrate the utility of these nanostructured surfaces for concentrating microscale magnetic beads, this system also should be compatible with nanoscale magnetic particles. In fact, beads with diameters closer to the size scale of the curvature of the nanopikes may be trapped more effectively by the magnetic gradients generated by each spike. Moreover, reducing the size of ECM-coated beads, in turn, reduces the area available to form cell adhesive sites. Based on studies of force–size relationships of cell adhesions to ECM [22,24], we expect that as bead size is decreased; cell tractional forces transmitted to individual beads will also decrease, thereby lowering the magnetic pulling force required to immobilize individual beads in presence of traction forces exerted by adherent cells.

Other methods for controlling cell positioning and spreading have been described in the context of reconfigurable cell-based processing devices [32]. However, the system described here offers several advantages, including comparative simplicity and flexibility, the ability to create large microarrays of cells that can be analyzed in parallel, and low cost and durability which are critical features for long-term commercial success. The magnetic ‘virtual substrate’ described here also allows for nearly unlimited array configurations, limited only by the resolution of the laser-etching process. Furthermore, because the cell-adhesive molecules are supplied by the removable magnetic beads, the user can easily specify the molecule used to mediate cell attachment for a given application. This same feature may be utilized in conjunction with other technologies such as microfluidics to create reconfigurable microarrays of magnetic microbeads-coated with biological molecules (e.g., DNA, proteins) in devices for genomic or proteomic applications.

A key element of this device is the ability to selectively control cell shape and viability by applying magnetic forces to cell-bound magnetic microparticles. The magnetic field gradients we created were sufficient to support increases in projected cell areas by at least 36%. This degree of cell distortion was large enough to prevent apoptosis, and the

level of survival increased when the intensity of the magnetic field was increased, thus confirming that even a small degree of cell distortion can prevent apoptosis in adherent cells, as previously described [1]. This magnetic shape-control capability may provide a way to induce cell death within future biodetectors that have been contaminated by a biological pathogen or toxin. Removal of the magnetic field would allow contaminated cells to be washed away and new magnetic beads and cells delivered to the same multiplexed islands (e.g., using microfluidics) to create a reconfigurable cell-based biochip detector system.

## 5. Conclusions

We have developed multiplexed magnetic field gradient concentrators that can be used in combination with magnetic microbeads coated with cell adhesion molecules to create ‘virtual culture substrates’. These biocompatible materials can be used to culture multiple cells in precise positions at high density, and to selectively induce cell death on command by removing an external magnet, thereby releasing cells to round up and die. Critical to this approach is the development of a method to fabricate arrays of magnetizable nanopikes that locally concentrate magnetic field gradients at the surface of the material, and thereby provide a way to trap these beads with sufficient force to resist high cell traction forces. Non-specific adhesive interactions with the remaining surface of the stainless steel substrate are inhibited by coating the material with a smooth layer of Pluronic detergent-treated PDMS. This simple system that has minimal power requirements and provides a reconfigurable interface for control of cell position and viability may be useful for future cell-based or biomolecule-based biodetectors, screening technologies, computers and other microsystems devices.

## Acknowledgments

This project was supported by DARPA Grant N000140210780 and support from the KECK Foundation.

## References

- [1] Chen CS, Mrksich M, Huang S, Whitesides GM, Ingber DE. Geometric control of cell life and death. *Science* 1997;276:1425–8.
- [2] Bhatia SN, Balis UJ, Yarmush ML, Toner M. Probing heterotypic cell interactions: hepatocyte function in microfabricated co-cultures. *J Biomater Sci Polym Ed* 1998;9:1137–60.
- [3] Singhvi R, Kumar A, Lopez GP, Stephanopoulos GN, Wang DI, Whitesides GM, et al. Engineering cell shape and function. *Science* 1994;264:696–8.
- [4] Gu W, Zhu X, Futai N, Cho BS, Takayama S. Computerized microfluidic cell culture using elastomeric channels and Braille displays. *Proc Natl Acad Sci USA* 2004;101:15861–6.
- [5] Zhu X, Yi Chu L, Chueh BH, Shen M, Hazarika B, Phadke N, et al. Arrays of horizontally-oriented mini-reservoirs generate steady

- microfluidic flows for continuous perfusion cell culture and gradient generation. *Analyst* 2004;129:1026–31.
- [6] Huh D, Gu W, Kamotani Y, Grotberg JB, Takayama S. Microfluidics for flow cytometric analysis of cells and particles. *Physiol Meas* 2005;26:R73–98.
- [7] Paddle BM. Biosensors for chemical and biological agents of defence interest. *Biosens Bioelectron* 1996;11:1079–113.
- [8] Tan W, Desai TA. Microfluidic patterning of cells in extracellular matrix biopolymers: effects of channel size, cell type, and matrix composition on pattern integrity. *Tissue Eng* 2003;9:255–67.
- [9] Tempelman LA, King KD, Anderson GP, Ligler FS. Quantitating staphylococcal enterotoxin B in diverse media using a portable fiber-optic biosensor. *Anal Biochem* 1996;233:50–7.
- [10] Okano T, Yamada N, Okuhara M, Sakai H, Sakurai Y. Mechanism of cell detachment from temperature-modulated, hydrophilic–hydrophobic polymer surfaces. *Biomaterials* 1995;16:297–303.
- [11] Elbert DL, Hubbell JA. Conjugate addition reactions combined with free-radical cross-linking for the design of materials for tissue engineering. *Biomacromolecules* 2001;2:430–41.
- [12] Schutt M, Krupka SS, Milbradt AG, Deindl S, Sinner EK, Oesterhelt D, et al. Photocontrol of cell adhesion processes: model studies with cyclic azobenzene-RGD peptides. *Chem Biol* 2003;10:487–90.
- [13] Jiang X, Ferrigno R, Mrksich M, Whitesides GM. Electrochemical desorption of self-assembled monolayers noninvasively releases patterned cells from geometrical confinements. *J Am Chem Soc* 2003;125:2366–7.
- [14] Yeo WS, Yousaf MN, Mrksich M. Dynamic interfaces between cells and surfaces: electroactive substrates that sequentially release and attach cells. *J Am Chem Soc* 2003;125:14994–5.
- [15] Shen MY, Crouch CH, Carey JE, Younkin R, Mazur E, Sheehy M, et al. Formation of regular arrays of silicon microspikes by femtosecond laser irradiation through a mask. *Appl Phys Lett* 2003;82:1715–7.
- [16] Tan JL, Liu W, Nelson CM, Raghavan S, Chen CS. Simple approach to micropattern cells on common culture substrates by tuning substrate wettability. *Tissue Eng* 2004;10:865–72.
- [17] Freedman DA, Folkman J. Maintenance of G1 checkpoint controls in telomerase-immortalized endothelial cells. *Cell Cycle* 2004;3:811–6.
- [18] Ingber DE, Prusty D, Frangioni JV, Cragoe Jr EJ, Lechene C, Schwartz MA. Control of intracellular pH and growth by fibronectin in capillary endothelial cells. *J Cell Biol* 1990;110:1803–11.
- [19] Ingber DE, Madri JA, Folkman J. Endothelial growth factors and extracellular matrix regulate DNA synthesis through modulation of cell and nuclear expansion. *In Vitro Cell Dev Biol* 1987;23:387–94.
- [20] Meyer CJ, Alenghat FJ, Rim P, Fong JH, Fabry B, Ingber DE. Mechanical control of cyclic AMP signalling and gene transcription through integrins. *Nat Cell Biol* 2000;2:666–8.
- [21] Flusberg DA, Numaguchi Y, Ingber DE. Cooperative control of Akt phosphorylation, bcl-2 expression, and apoptosis by cytoskeletal microfilaments and microtubules in capillary endothelial cells. *Mol Biol Cell* 2001;12:3087–94.
- [22] Balaban NQ, Schwarz US, Riveline D, Goichberg P, Tzur G, Sabanay I, et al. Force and focal adhesion assembly: a close relationship studied using elastic micropatterned substrates. *Nat Cell Biol* 2001;3:466–72.
- [23] Matthews BD, Overby DR, Alenghat FJ, Karavitis J, Numaguchi Y, Allen PG, et al. Mechanical properties of individual focal adhesions probed with a magnetic microneedle. *Biochem Biophys Res Commun* 2004;313:758–64.
- [24] Tan JL, Tien J, Pirone DM, Gray DS, Bhadriraju K, Chen CS. Cells lying on a bed of microneedles: an approach to isolate mechanical force. *Proc Natl Acad Sci USA* 2003;100:1484–9.
- [25] Matthews BD, Overby DR, Mannix R, Ingber DE. Cellular adaptation to mechanical stress: role of integrins, Rho, cytoskeletal tension and mechanosensitive ion channels. *J Cell Sci* 2006;119:508–18.
- [26] Overby DR, Matthews BD, Alsberg E, Ingber DE. Novel dynamic rheological behavior of individual focal adhesions measured within single cells using electromagnetic pulling cytometry. *Acta Biomater* 2005;1:295–303.
- [27] Chicurel ME, Singer RH, Meyer CJ, Ingber DE. Integrin binding and mechanical tension induce movement of mRNA and ribosomes to focal adhesions. *Nature* 1998;392:730–3.
- [28] Li YS, Haga JH, Chien S. Molecular basis of the effects of shear stress on vascular endothelial cells. *J Biomech* 2005;38:1949–71.
- [29] Wang Y, Botvinick EL, Zhao Y, Berns MW, Usami S, Tsien RY, et al. Visualizing the mechanical activation of Src. *Nature* 2005;434:1040–5.
- [30] Kip AF. *Fundamentals of Electricity and Magnetism*. New York: McGraw-Hill Book Company; 1962.
- [31] Shen MY, Crouch CH, Carey JE, Mazur E. Femtosecond laser-induced formation of submicrometer spikes on silicon in water. *Appl Phys Lett* 2004;85:5694–6.
- [32] Zhu X, Mills KL, Peters PR, Bahng JH, Liu EH, Shim J, et al. Fabrication of reconfigurable protein matrices by cracking. *Nat Mater* 2005;4:403–6.